Article

Determination of the Composition of Bio-Oils from the Pyrolysis of Orange Waste and Orange Pruning and Use of Biochars for the Removal of Sulphur from Waste Cooking Oils

Francisco-José Sánchez-Borrego [ID], Noelia García-Criado, Juan F. García-Martín *[ID] and Paloma Álvarez-Mateos *[ID]

Departamento de Ingeniería Química, Facultad de Química, Universidad de Sevilla, C/Profesor García González s/n, 41012 Seville, Spain; fsanchez25@us.es (F.-J.S.-B.); noegarcri@gmail.com (N.G.-C.)
* Correspondence: jfgarmar@us.es (J.F.G.-M.); palvarez@us.es (P.Á.-M.)

Abstract: Waste generated in the agri-food sector is a potential source of biomass and other products of high added value. In this work, the pyrolysis of orange waste and orange pruning was carried out to produce adsorbent biochars and characterise the bio-oils aiming for high-added-value compounds. Pyrolysis was carried out in a vertical tubular furnace on the laboratory scale modifying the temperature (400–600 °C), the heating ramp (5–20 °C·min^{-1}) to reach the previous temperature and the inert gas flow rate (30–300 mL Ar·min^{-1}) throughout the furnace. The most suitable conditions for obtaining biochar were found to be 400 °C, 5 °C·min^{-1}, and 150 mL Ar·min^{-1} for orange waste, and 400 °C, 10 °C·min^{-1}, and 150 mL Ar·min^{-1} for orange pruning. Thermogravimetric analysis showed higher thermal stability for orange pruning due to its higher lignin content (20% vs. 5% wt. on a wet basis). The bio-oil composition was determined by GC-MS. Toluene and 5-hydroxymethylfurfural were the main compounds found in orange waste bio-oils, while orange pruning bio-oils were composed mainly of 4-hydroxy-4-methyl-2-pentanone. Finally, the removal of the sulphur content from waste cooking oil was assayed with the biochars from both orange waste and orange pruning, whose BET surface areas were previously determined. Despite their low specific surface areas (≤ 1 m^2·g^{-1} for orange waste biochars and up to 24.3 m^2·g^{-1} for orange pruning biochars), these biochars achieved a reduction of the initial sulphur content of the waste cooking oil between 66.4% and 78.8%.

Keywords: biochar; bio-oil; oil desulphurisation; orange pruning; orange waste; pyrolysis

1. Introduction

Among all raw materials in the food industry, fruits and vegetables produce the most waste. In Europe, Spain leads the orange and orange juice production ranking, and is sixth in the global ranking, according to the Food and Agriculture Organization (2018) [1]. In Spain, this agricultural activity can be found mainly in Valencia and Andalusia, producing almost 2×10^6 t per year of sweet oranges, the fruit of the sweet orange tree (*Citrus sinensis*). According to the Spanish Ministry of Agriculture, Fishing, and Food [2], the orange harvesting, handling, transport, and marketing are responsible for thousands of jobs [3].

Farmers prune to remove old branches and regenerate orange trees. In Spain, more than 5×10^6 t of orange pruning are produced annually, which are considered as waste and therefore must be disposed of to avoid contamination, pest growth, and delay in agricultural practices [4]. As a lignocellulose material, orange-tree pruning is mainly composed of cellulose, hemicellulose, and lignin.

The citrus industry, in particular the orange juice sector, produces more than 2.2×10^6 t of waste in Spain each year [2]. The orange waste (OW) generated in the production of orange juice accounts for around 50–60 wt.% in wet basis [5] of the processed fruit, with an amount of moisture of approximately 82% wt.% [6], the waste containing approximately 60–65% peel, 30–35% pulp, and 0–10% seeds [7]. These residues have no profitable

commercial use. Traditionally, they are used for animal feed, as fertiliser [8], or as cattle bedding, options that provide no benefit either economically or for the environment, so many of them go to dumps, creating a logistic problem [9] and increasing the economic and environmental problems [10].

Therefore, a profitable alternative for these orange residues is needed. In recent years, different recovery and reuse pathways have been proposed. Among them, biochemical processes such as fermentation for bioethanol production [11], anaerobic digestion [12,13], and recovery of flavonoids and chemical products [14] are highlighted. Recently, thermal conversion methods, such as gasification, roasting, pyrolysis [15], and catalytic hydrotreating [16] have also been researched.

Pyrolysis is one of the main thermochemical processes for converting biomass into valuable products [17]. It is the thermal degradation of organic material in the absence of oxygen. During the pyrolysis process, each lignocellulose material undergoes different reaction mechanisms (i.e., decarboxylation, dehydration, and demethylation), resulting in biochar, bio-oil, and syngas production [18]. Pyrolysis can be fast or slow, depending mainly on the heating ramp and residence time, and other factors such as pressure and the type of process (batch or continuous) [19]. The performance, composition, and distribution of the products depend on the pyrolysis conditions, mainly on factors such as the nature of the biomass (starting raw material), previous treatments, particle size, reactor type, maximum reaction temperature, heating ramp, residence time, pressure, use of a mineral catalyst, etc. [20]. Lower process temperatures and heating ramps and longer gas residence times improve biochar production [21]. Approximately 35% of the weight of dry biomass can be turned into biochar, although higher pressures can provide significantly higher performance.

The liquid part, bio-oil, is a dark brown polar fluid that flows freely and is similar to biomass in its elemental composition. It is composed of a very complex mixture of oxygenated derivatives of hydrocarbons, which result from the incomplete degradation of long-chain hydrocarbons, cellulose, hemicellulose, and part of lignin, which is decomposed during pyrolysis into smaller and lighter molecules, such as tars, oils, phenols, and waxes [17]. It has a distinctive smoky smell due to the presence of low-molecular-weight aldehydes and acids. The bio-oil from orange peel contains valuable compounds such as phenols, benzenes, toluene, p-xylene, styrene, carboxylic acid, and d-limonene (its main component) [21]. D-limonene can be used in the food and pharmaceutical industries. As for bio-oils from the pyrolysis of orange pruning, no data is available in the literature.

Non-condensable gases (syngas) are a mixture of basic components such as carbon monoxide (CO) and hydrogen (H_2). Their higher heating value has been reported to be 4.37–5.68 MJ/m^3 [21]. Both bio-oil and syngas have the heating potential to be used as a cogeneration energy source in biomass waste pyrolysis plants.

Biochar is a non-volatile solid waste rich in carbon, composed of the remaining biomass that is not hydrocarbons, mainly parts of lignin, oxides (usually metallic), and heavy metals, depending on the composition of the raw material. It is used as fuel (briquettes) [22], as an alternative adsorbent to remove different types of contaminants, including heavy metals, nutrients, and pharmaceuticals from aqueous solution [23], as an amendment to improve soil fertility, as a raw material for the preparation of activated carbon [24] and, mainly, as a biocatalyst. For example, biochars from different raw materials were used to catalyse the esterification reaction of free fatty acids with methanol [25–27] or with glycerol [28], and the esterification of glycerol with acetic acid or acetic anhydride [29], all of them within the biodiesel production framework.

The sulphur content in fuels is of major importance due to the formation of sulphur oxides during fuel combustion in engines, which in turn react with water steam to produce sulphuric acid. Regarding biodiesel, its maximum sulphur content as established by the EN14214 standard is 10 mg·kg^{-1}. This is of great importance for companies dealing with the recycling of waste cooking oils (WCO). Thus, the sale price of the WCO of these companies to biodiesel industries depends on the sulphur content [30]. Sulphur removal in vegetable

oils and WCO has been studied mainly in relation to the subsequent biodiesel production, considering the above-mentioned environmental problems associated with SO_x emissions and the corrosion in the engines [30]. The most widely used treatments for sulphur removal are adsorption, solvent extraction, precipitation, and oxidation reaction [31]. As previously stated, biochars can act as adsorbent. Hence, they could be used for the removal of sulphur in WCO. To the best of our knowledge, this possibility has not been explored yet. Based on all the aforementioned considerations, the objectives of this work were the following:

(1) Valorising orange tree pruning and sweet orange waste (currently used for the production of boiler pellets and cattle feed, respectively) through the production of biochar and bio-oil by slow pyrolysis.
(2) Characterise the biochars and bio-oils obtained.
(3) Apply the biochars obtained for the removal of sulphur from waste cooking oils.

2. Materials and Methods

2.1. Raw Materials

The company Export Orange S.L. (Salteras, Spain) provided orange tree pruning (OP) and sweet oranges (SO), while Grupo BIOSEL S.L. (Aznalcóllar, Spain) supplied the waste cooking oil (WCO) used throughout this research.

2.2. Pretreatment of Sweet Oranges

SO were weighted, superficially washed with distilled water, dried, and ground in a Thermomix TM 21 (Vorwerk, Wuppertal, Germany) to obtain 1×1 cm section. Subsequently, the juice was separated from the peel and the pulp by sieving. Afterward, the mixture of peel and pulp (orange waste, OW) was dried at 45 °C in a laboratory oven. Most of the moisture (80% wt.) of the OW was removed. The OW was then weighed, ground in a ball mill at 500 rpm for 20 min, and passed through a sieve to achieve a particle size of less than 1 mm. Finally, the OW was dried in the oven at 45 °C.

2.3. Pretreatment of Orange Pruning

First, the leaves were separated from the branches, and then the latter (OP) were chopped and introduced in an oven at 45 °C. Subsequently, the OP was milled in a ball mill at 500 rpm for 20 min to achieve a particle size of less than 1 mm and introduced again in the oven at 45 °C until constant weight.

2.4. Pyrolysis

OW and OP were subjected to thermal treatment under an inert atmosphere (Ar). Pyrolysis was carried out in a vertical tubular pyrolytic furnace (16 cm height, 3.5 cm diameter). The reactor was a quartz tube with a porous plate and a ground nozzle, into which 9 g of OW or 4.33 g of OP, respectively, were introduced (Figure 1).

The heating ramp was programmed using a CN300-P temperature regulator (Conatec, Irún, Spain), connected to the oven through a thermocouple. A heating wire was placed around the bottom of the quartz tube (supported by aluminum foil) to prevent condensation of the liquid in the tube, which was intended to occur in the round bottom flask (Figure 1). Two ethanol traps were used to remove pollutants from syngas. A rotameter was used to control the flow rate of the inert gas (Ar) through the pyrolysis reactor.

The operational variables to study were the flow rate of the inert gas (30, 150, and 300 mL Ar·min^{-1}), the maximum pyrolysis temperature (400 and 600 °C) and the heating ramp (5, 10 and 20 °C·min^{-1}), maintaining the maximum temperature for 2 h. Subsequently, the system was cooled to room temperature. These conditions were selected based on previous work on citrus pyrolysis available in the literature [15,20,32–34]. Each experiment was carried out in duplicate. The experimental set of pyrolysis carried out is illustrated in Table 1.
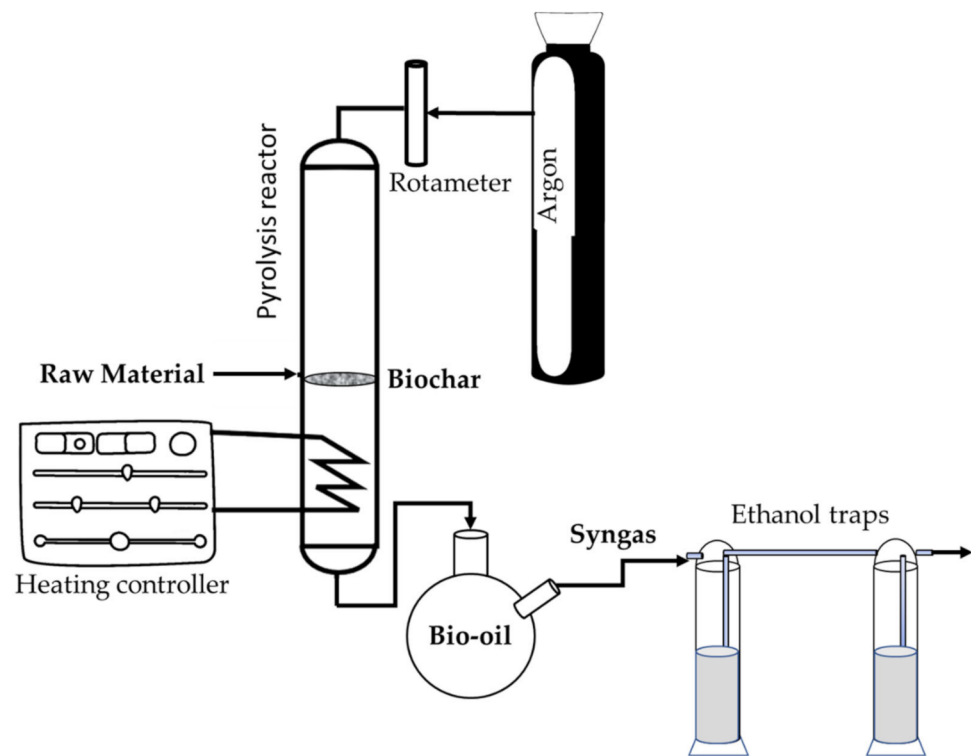
Figure 1. Pyrolysis equipment.

Table 1. Pyrolysis conditions for orange pruning (OP) and orange waste (OW).

Raw Material	Initial Mass (g)	T (°C)	H_{ramp} (°C·min^{-1})	Ar Flow Rate (mL·min^{-1})
OW	9.00	400	5	150
OW	9.00	400	10	150
OW	9.00	600	10	30
OW	9.00	600	10	150
OW	9.00	600	10	300
OP	4.33	400	5	150
OP	4.33	400	10	150
OP	4.33	600	10	30
OP	4.33	600	10	150
OP	4.33	600	10	300
OP	4.33	600	20	150

H_{ramp}: heating ramp.

2.5. Adsorption of Sulphur in Oils by the Produced Biochars

The study of the sulphur adsorption by the biochars was carried out in a 250 mL stirred batch reactor, in which 50 mL WCO were introduced along with 5 g biochar (10% w/v). The temperature, stirring and residence time were set to 50 °C, 700 rpm and 120 min, respectively. All the experiences were carried out in duplicate. Subsequently, the biochar was removed from the WCO by filtration, and the sulphur content in the oil was analysed.

2.6. Products Characterisation

2.6.1. Thermogravimetric Analysis

Thermogravimetric analysis was used to determine the lignin, hemicellulose, and cellulose content of the samples and to obtain information on the optimal carbonisation temperature. To perform the analysis, an SDT Q600 electrobalance (TA Instruments, Inc., New Castle, DE, USA) with a sensitivity of +/− 0.5 μg was used. The sample heating system consisted of a vertical furnace capable of reaching a maximum temperature of 1200 °C.

The samples were first heated under an Ar atmosphere to decompose the organic matter, leaving only inorganic ash. The analyses were carried out at a 10 °C·min^{-1} constant heating ramp until reaching 800 °C under a flow rate of 100 mL Ar·min^{-1} until constant weight.

2.6.2. Fourier-Transform Infrared Spectroscopy (FTIR)

A Nicolet iS5 FTIR spectrometer (Thermo Fisher Scientific, Waltham, MA, USA) was used to characterise the raw materials as well as the biochars obtained before and after the desulphurisation of WCO. The powder compaction was carried out on a uniaxial press applying a pressure of 10 t·cm^{-2}. For transmission measurements, 13 mm capsules were prepared using potassium bromide (KBr) as diluent, 5% wt. being the final sample concentration. Spectra were recorded in the 500–4000 cm^{-1} range.

2.6.3. Biochar Texture Characterisation

The BET method was used to calculate the specific surface area (SBET). A Gemini V-2365 adsorption equipment (Micromeritics Instrument Corporation, Norcross, GA, USA) was used. The biochars were previously degassed at 170 °C for 2 h under N_2 atmosphere.

2.6.4. Gas Chromatography–Mass Spectrometry

A qualitative analysis of the bio-oil composition from pyrolysis was performed with a TSQ8000 mass spectrometer (Thermo Fisher Scientific, Waltham, MA, USA) coupled to a triple quadrupole gas chromatograph (GC-MS), equipped with an autosampler. A Zebron ZB-5MS column (30 m × 0.25 mm × 0.25 μm; 5% phenyl-arylene, 95% dimethylpolysiloxane) and N_2 as carrier gas were used. Analyses were carried out under the following conditions: 50 °C initial temperature, 7 °C·min^{-1} heating ramp for 30 min, and final temperature of 310 °C.

The identification of the peaks was performed using the database of the Quan Browser tool of the XCalibur software (Thermo Fisher Scientific, Waltham, MA, USA). To limit the compounds, several factors were taken into account: that the area of the compound had a value greater than 1, that the probability of the compound was greater than 40%, and that the compound were present in a greater number of samples. The area of each compound was calculated using the internal standard method.

2.6.5. Determination of Sulphur in Oils

The WCO samples were subjected to acid digestion in a microwave digestion system (UltraWAVE, Milestone Inc., Santa Clara, CA, USA). Briefly, 0.25 g WCO were weighted and digested in 25 mL closed glass beakers at 200 °C with 4 mL HNO_3 and 1 mL H_2O_2, to finally making up to a volume of 25 mL with distilled water. After digestion, the sulphur content in the samples was determined using a Spectroblue TI (Spectro Analytical Instruments GmbH, Kleve, Germany) inductively coupled plasma-optical emission spectrometer.

3. Results and Discussion

3.1. Characterisation of the Raw Material

Thermogravimetric Analysis (TGA)

Three stages of mass loss were observed in the TGA or orange pruning (Figure 2A). The first stage was related to moisture removal, which could be divided in turn into two stages: one until 92 °C (4 wt.%) and the other until 120 °C, suggesting the presence of at least two types of water bonding in the samples. The latter (8% mass loss) was related to adsorbed water molecules, weakly linked by hydrogen bonds. The second stage of mass loss, which ranges from 130 to 210 °C and reached a mass loss of 41%, is the active zone, generally related to the degradation of hemicellulose and cellulose polymers [35]. The third stage of mass loss, from 210 to 600 °C, is the passive zone, attributed to lignin decomposition, with the highest mass loss occurring between 210 and 300 °C.
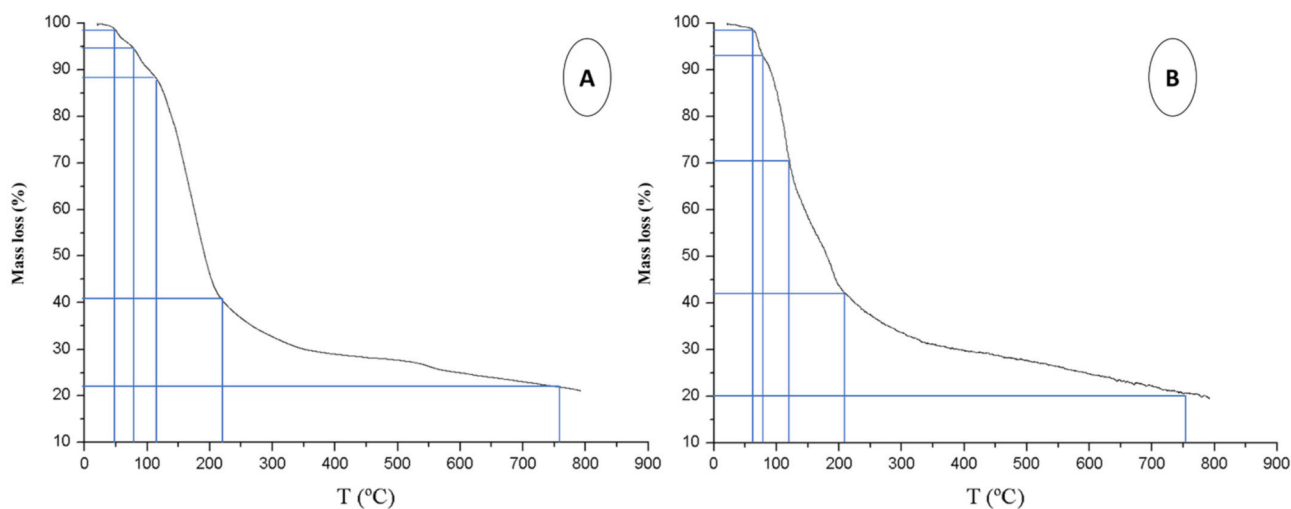
Figure 2. Thermogravimetric curve obtained in the pyrolysis of orange tree pruning (**A**) and orange waste (**B**).

Assuming the data depicted in Figure 2A, the lignin content could account for 20 wt.%, taking into account the large limitations of TGA for quantitative analysis. Beyond this stage, the mass loss up to 800 °C can be attributed to the total degradation of the biomass. The non-degraded remaining mass at 800 °C could correspond to inorganic salts.

Similarly to what occurred for OP, mass loss up to roughly 100 °C in the TGA of orange waste was associated with moisture removal. Again, a slope close to 73 °C and another close to 114 °C were observed, corresponding to physically absorbed and adsorbed water molecules, respectively (Figure 2B). There was also another mass loss due to pectin water ranging from 87 to 165 °C, which corresponds to a mass loss of 36% [36]. Therefore, the sample had approximately 45 wt.% moisture.

Cellulose and hemicellulose polymers degraded between 165 and 205 °C for OW and showed a maximum degradation rate at 188 °C, as observed in Figure 2B. In the literature, studies carried out on sweet oranges and under the same conditions assume that cellulose and hemicellulose begin their degradation together, presenting a maximum degradation rate at 213 °C. This trend was also noted in the study of the pyrolysis of six species of tropical hardwoods under an N_2 atmosphere [37].

According to the literature, cellulose degrades between 315 and 400 °C [36], and hemicellulose begins its degradation at a slightly lower temperature (220–315 °C), due to the more disordered nature of the polymer [38]. From the thermogravimetric curve (Figure 2B), it could be assumed that the degradation of cellulose and hemicellulose began at 165 °C and ended at 205 °C, corresponding to a loss of mass of 14%. Pectin degradation showed several continuous and prolonged weight losses at various temperatures (226, 305, 394, and 475 °C) [34]. In this case, pectin would degrade between approximately 205 and 400 °C, leading to various weight losses (overlapping peaks). This range would correspond to a loss of mass of 12 wt.%, according to the literature [35].

In Figure 2B, the lignin degradation process began at room temperature and gradually degrades up to 800 °C [36], a temperature at which 80 wt.% decomposition of the initial mass was reached. It would correspond to a lignin content of roughly 5% wt. At 800 °C, 20 wt.% raw material would remain undegraded, which corresponds to carbon residues and metallic compounds. The ash content was 3 wt.%, a value that agrees with the data available in literature [7].

In summary, the greatest weight loss occurred up to 400 °C (Figure 2A,B), which indicates that the samples are mainly made up of water, cellulose, and hemicellulose, while 72–78% degradation of the initial mass was achieved at 600 °C, which coincides with what is reported in the literature [38].

3.2. Product Distribution after Pyrolysis

The bio-oils and biochars obtained were weighed to obtain their percentages after pyrolysis (Table 2). The biochars obtained were stored in individual containers. Subsequently, the BET specific surface area (S_{BET}) of each biochar was measured, and the FTIR spectra were acquired. The bio-oils were analysed by GC-MS.

Table 2. Material balance of the performed pyrolyses.

Raw Material	T (°C)	H_{ramp} (°C·min^{-1})	Ar Flow Rate (mL·min^{-1})	Biochar (% wt.)	Bio-Oil (% wt.)	Syngas (% wt.)	S_{BET} (m^2/g)
OW	400	5	150	37.7	57.8	4.6	≤1
OW	400	10	150	34.3	56.7	7.9	≤1
OW	600	10	30	32.1	56.6	11.2	≤1
OW	600	10	150	31.3	58.9	9.8	≤1
OW	600	10	300	30.9	62.2	6.9	≤1
OP	400	5	150	35.1	58.2	6.7	2.8
OP	400	10	150	35.3	57.3	7.4	5.4
OP	600	10	30	24.7	67.2	8.1	24.3
OP	600	10	150	27.9	65.6	6.5	9.6
OP	600	10	300	29.1	57.5	13.4	12.0
OP	600	20	150	28.2	55.2	16.6	10.4

OW: orange waste; OP: orange pruning; H_{ramp}: heating ramp; S_{BET}: BET-specific surface.

The trends reported by other authors can be observed in Table 2 for OW biochars [15,39]. At 400 °C, moving from different heating ramps (5 and 10 °C·min^{-1}), there is a decrease in the percentages obtained of biochar and bio-oil, as well as an increase in syngas with the increase in the ramp. In contrast, at 400 °C and different heating ramps (5 and 10 °C·min^{-1}), the percentages remain stable for the OP biochar samples.

For OW biochars, at different pyrolysis temperatures (400 and 600 °C), there is a decrease in biochar percentages and an increase in biogas when the temperature is higher (Table 2). No significant differences were observed in the bio-oil percentages. Furthermore, for OP biochars, at 600 °C, there was a higher bio-oil proportion and less biochar than those produced at 400 °C. In general, the percentage of biochar decreases and those of the fluids increase as the temperature increases. This trend is in agreement with the available literature using orange peel [40] or coffee silverskin [41].

When increasing the flow rate of the inert gas (30, 150, and 300 mL Ar·min^{-1}), a decrease in the percentages of biochar and syngas (and therefore an increase in bio-oil) is observed for OW, as Charusiri et al., pointed out in the pyrolysis of sugarcane leaves [40]. On the contrary, as Ar flow increases in OP pyrolysis at 600 °C and 10 °C·min^{-1}, the percentages of syngas and biochar also increase, thus decreasing the bio-oil fraction.

Finally, for OP pyrolysis at 600 °C with the same Ar flow (150 mL·min^{-1}), as the heating ramp increases, the percentage of biochar does not change, bio-oil decreases, and syngas increases. A low heating ramp implies an enhanced heat transfer [41]; this could be the reason why the percentage of bio-oil decreases as the heating ramp increases, because the degradation of the raw material is lower.

3.3. Characterisation of Biochars

3.3.1. Temperature Influence

In order to assess the effect of temperature, the FTIR spectra of the raw materials were compared with those of the biochars obtained from OW and OP at different maximum pyrolysis temperatures, one at 400 °C and the other at 600 °C, keeping in both cases the rest of the conditions constant (Figure 3).
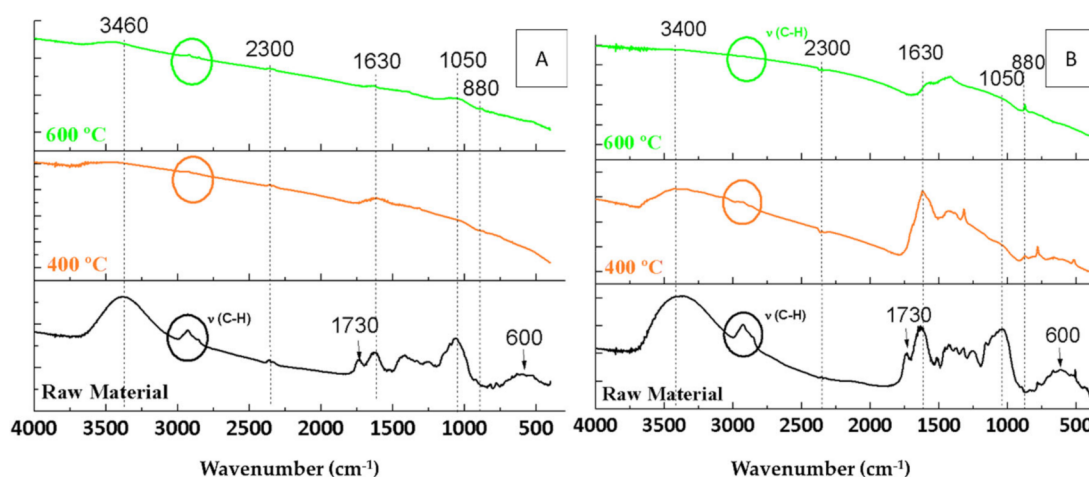
Figure 3. FTIR spectra of the raw materials and the biochars resulting from the pyrolyses under 150 mL Ar·min^{-1} flow rate and 10 °C·min^{-1} heating ramp for 2 h of orange waste (**A**) and orange pruning (**B**) at different temperatures.

Regarding the OW biochars, it was observed that thermal treatment led to a decrease in the intensity of the FTIR bands present in the raw material. Bands associated with the presence of water adsorbed on the surface (a wide band around 3400 cm^{-1} and a band at 1630 cm^{-1}) decreased considerably in OW biochars (Figure 3A). These bands shifted slightly towards higher wavenumbers after pyrolysis. For example, the water band observed at 3380 cm^{-1} for OW could be found at 3640 cm^{-1} in its biochars (indicated by an arrow in Figure 3A).

In addition to water, it was observed that the C-H vibration bands in the C-H vibrations region (2900 cm^{-1}) [24] were more intense for the highest pyrolysis temperature (600 °C), which could indicate that a hydrocarbon skeleton may be formed at this temperature. The band at 2300 cm^{-1} corresponds to the asymmetric tension vibration of the CO_2 molecule. Although its intensity was low in the raw material, it decreased with an increase in the pyrolysis temperature.

Furthermore, with respect to OP biochars (Figure 3B), the bands related to water (3400 and 1630 cm^{-1}) at 400 °C had a smaller decrease in intensity, while at 600 °C, they completely disappeared. In addition to water, the band in the C-H vibrations region (2900 cm^{-1}) [24] was more intense for the lowest pyrolysis temperature, which could indicate that a hydrocarbon skeleton may be formed at this temperature. The band at 2300 cm^{-1} (CO_2) remained almost constant. Finally, for both OP and OW biochars, the band attributed to C=O bonds (for example of lactones) at 1730 cm^{-1} disappeared completely after pyrolysis, as did the band that corresponds to calcium compounds (600 cm^{-1}), due to their decomposition with increasing temperature [34]. Finally, the intensity of the band at 880 cm^{-1}, corresponding to aromatic compounds [35], increased with increasing temperature.

3.3.2. Influence of the Inert Gas Flow Rate

To evaluate the influence of flow, the FTIR spectra of the raw materials were compared with those of the biochars obtained from OW and OP at different flow rates, namely 30, 150, and 300 mL Ar·min^{-1}, maintaining constant the rest of the pyrolysis conditions (Figure 4).
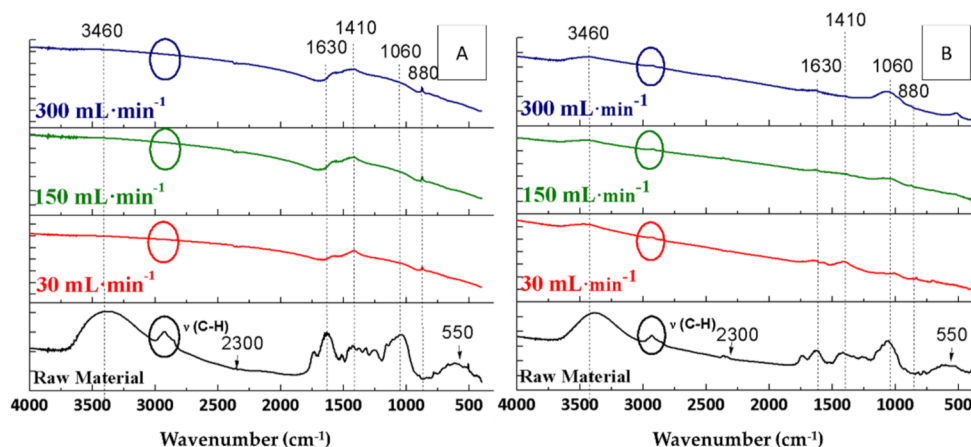
Figure 4. FTIR spectra of the raw materials and the biochars resulting from pyrolyses of orange waste (**A**) and orange pruning (**B**) carried out at 600 °C for 2 h with a heating ramp of 10 °C·min^{-1} using different Ar flow rates.

Regarding orange waste, the water bands (3460 and 1630 cm^{-1}) of the resulting biochars had the same intensity under the three assayed conditions (Figure 4A). It was remarkable that the bands in the region of the C-H vibrations (at 2900 cm^{-1}) [24] were only found at higher flow rates, whereas the band at 2300 cm^{-1} (CO_2) did not depend on the flow rate. The intensity of the band at 1410 cm^{-1} (carboxylic acid band) [42] was inversely proportional to the flow rate. Therefore, the highest intensity was observed in the experience carried out under 30 mL Ar·min^{-1} flow rate (Figure 4A). In contrast, of note is that the intensity of the 1060 cm^{-1} band (C-O bond) was directly proportional to the flow rate, corresponding to the band that appeared with the highest intensity in the biochar pyrolysed under 300 mL Ar·min^{-1}. The band at 880 cm^{-1}, corresponding to aromatic compounds [37], did not appear in the OW biochars. Finally, the band related to calcium was observed at 550 cm^{-1} [43], which only appeared in OW biochars when working under 300 mL Ar·min^{-1}.

On the other hand, with respect to the OP biochars, the band at 3460 cm^{-1} was barely noticeable, while there was a small band at 1630 cm^{-1}. The band at 2900 cm^{-1} disappeared completely. Similarly to OW biochars, the band at 2300 cm^{-1} (CO_2) was not related to the assayed flow rate during the pyrolysis process. The band at 1730 cm^{-1} completely disappeared from the OP after pyrolysis. The band at 1410 cm^{-1} was also inversely proportional to the flow rate. However, there were no differences in the band at 1060 cm^{-1} in the FTIR spectra of the three biochars. Finally, the band at 880 cm^{-1}, which appeared after pyrolysis, could be seen in the FTIR spectra of OP biochars, while the band at 550 cm^{-1} did not appear.

3.3.3. Influence of the Heating Ramp

To study the influence of the heating ramp, the FTIR spectra of the raw materials were compared with those of the OW and OP biochars (Figures 5 and 6) obtained at different heating ramps, to be specific, 5, 10, and 20 °C·min^{-1}, keeping the rest of the conditions constant.
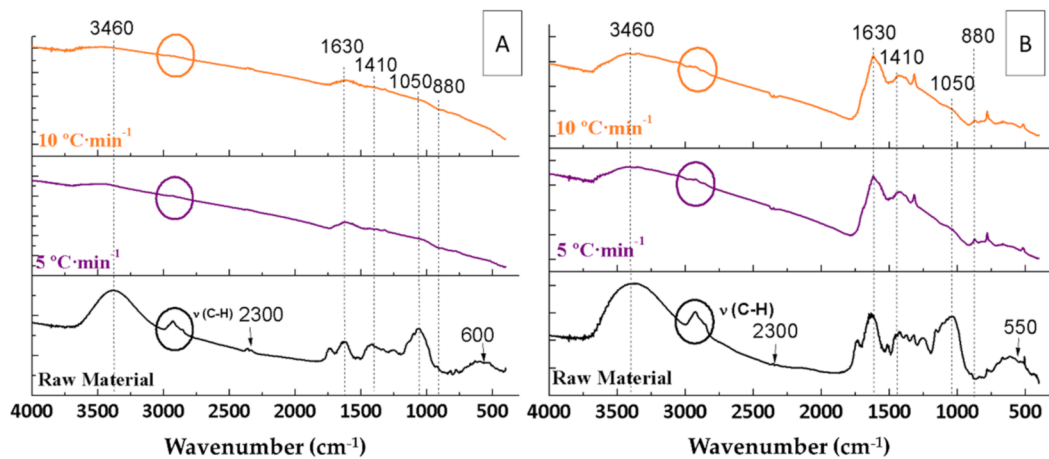
Figure 5. IR spectra of the raw materials and the biochars resulting from the pyrolyses of orange waste (**A**) and orange pruning (**B**) performed at 400 °C for 2 h under 150 mL Ar·min^{-1} flow rate using different heating ramps.
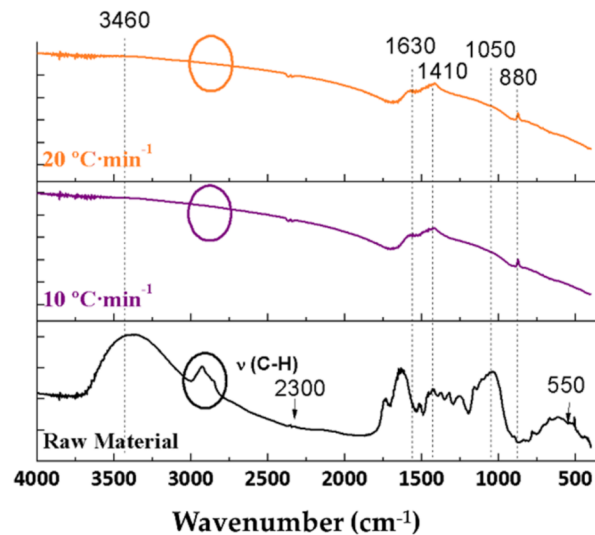
Figure 6. FTIR spectra of the raw material and the biochars resulting from the pyrolyses of orange pruning performed at 600 °C for 2 h under 150 mL Ar·min^{-1} flow rate using different heating ramps.

All bands marked in Figures 5 and 6 and described in Sections 3.3.1 and 3.3.2 were not affected by varying the flow rate. These bands included the bands at 3460 and 1630 cm^{-1} (water), at 2900 cm^{-1} (C-H), at 2300 cm^{-1} (CO_2), at 1730 cm^{-1} (C=O), at 1410 cm^{-1} (carboxylic acid), at 1060 cm^{-1} (C-O), at 880 cm^{-1} (aromatic), and at 550 cm^{-1} (Ca).

From the results, it can be concluded that the heating ramp and Ar flow rate do not influence the surface compounds, as they are solely influenced by the pyrolysis temperature.

Table 3 summarises the general vibration characteristics and wavenumbers of the compounds present in the FTIR spectra of the raw materials and the resulting biochars, comparing them to the literature [35].

Table 3. Main vibrations of the compounds present in the FTIR spectra of raw materials and biochars.

Group	Vibration	Experimental (cm^{-1})	Literature (cm^{-1})	Reference
Carboxylic acid and water	ν (O-H)	3600–3100, 1630	3600–3000, 1632	[35]
Alkyl, aliphatic, and aromatic	ν (C-H)	2925, 2860, 1400	2970–2860, 1402	[35]
Ketone and carbonyl	ν (C=O)	1730–1713, 1560	1730–1700, 1560–1510	[35]
Carboxylic acid	ν (O-H)	1410	1440–1400	[42]
Ether	ν (C-O)	1064–1000	1300–1000	[42]
Aromatic hydrogens	ν (C-H)	880–800	700–900	[44]
Calcium	ν (Ca-O)	550–600	550–600	[43]

3.4. Bio-Oil Characterisation

The bio-oils obtained were characterised using a gas chromatograph coupled to a mass spectrometer in order to perform a tentative qualitative analysis of the major compounds present in the resulting bio-oils under different pyrolysis conditions.

3.4.1. Temperature Influence

To assess the effect of temperature, the chromatograms of the bio-oils obtained from OW and OP at different pyrolysis temperatures, namely 400 and 600 °C, were compared (Tables 4 and 5, respectively), keeping constant in both cases the rest of the conditions (150 mL Ar·min^{-1}, 10 °C·min^{-1}, 2 h).

Table 4. Compounds detected in bio-oils chromatograms and their relative area percentages obtained in the pyrolysis of orange waste at different temperatures.

	Pyrolysis Temperature (°C)	
Compound	**600**	**400**
	Area (%)	
Propanoic acid	2.97	3.84
Toluene	24.63	29.43
2,4-Dimethyl-2-oxazoline-4-methanol	8.57	4.88
Furfural	2.98	8.09
2-Pentanone, 4-hydroxy-4-methyl-	3.08	5.94
2-Furanmethanol	3.17	2.70
2,5-Furandione, dihydro-3-methylene-	1.63	-
2-Furancarboxaldehyde, 5-methyl-	4.07	6.19
Phenol	3.00	2.41
Maltol	1.66	1.31
Pyranone	2.31	2.83
5-Hydroxymethylfurfural	23.01	32.37
4-Hydroxy-3-methylbenzoic acid, methyl ester	5.80	-
1-Methyl-8-propyl-3,6-diazahomoadamantan-9-ol	2.53	-
9-Octadecenamide, (Z)-	2.92	-
Hexadecanoic acid, 2-hydroxy-ethyl ester	5.18	-
Octadecanoic acid, 2,3-dihydroxypropyl ester	2.50	-

Table 4 shows the values of the areas and the main compounds in the chromatograms of bio-oils obtained in the pyrolysis of OW at 400 and 600 °C. Both bio-oils presented toluene and 5-hydroyxymethylfurfural (HMF) as the components of the highest intensity and area, these areas being higher at the lowest temperature (400 °C).

In the experience at 600 °C, the third major compound was 2,4-dimethyl-2-oxazoline-4-methanol. However, in the experience at 400 °C, the same compound had a much smaller area. Finally, furfural was identified, the concentration of which was higher in bio-oil obtained at 400 °C.

Table 5. Compounds detected in bio-oils chromatograms and their relative area percentages obtained in the pyrolysis of orange pruning at different temperatures.

Compound	Pyrolysis Temperature (°C)	
	600	400
	Area (%)	
Toluene	2.15	2.6
3-Penten-2-one, 4-methyl-	1.85	-
2-Pentanone, 4-hydroxy-4-methyl-	94.73	92.62
2-Furanmethanol	-	1.29
Phenol, 2-methoxy-	-	1.24
Phenol, 2,6-dimethoxy-	1.27	2.25

Table 5 shows the values of the areas and the main compounds in the chromatograms of bio-oils obtained in the pyrolysis of OP at 400 and 600 °C. The main compounds detected were 4-hydroxy-4-methyl-2-pentanone and toluene. Although the area of the first was higher at 600 °C, the area of the second was higher in the bio-oil obtained at 400 °C. However, the differences between the two experiences were very small.

Furthermore, the differences between the compounds obtained from each raw material were great (Tables 4 and 5). The main compound found in OP bio-oils was 4-hydroxy-4-methyl-2-pentanone, while the main compounds in OW bio-oils were toluene and furfural-related compounds.

3.4.2. Influence of Argon Flow Rate

In order to evaluate the influence of the atmosphere under which pyrolysis was performed, the GS-MS chromatograms of the bio-oils obtained from OW (Table 6) and OP (Table 7) using different inert gas flow rates (30, 150, and 300 mL Ar·min^{-1}) during the pyrolysis process have been compared, keeping the rest of the conditions (600 °C, 10 °C·min^{-1}, 2 h) constant in all three cases.

Table 6. Compounds detected in orange waste bio-oils chromatograms and their relative area percentages using different argon flow rates during the pyrolysis.

Compound	Argon Flow Rate (mL·min^{-1})		
	300	150	30
	Area (%)		
Propanoic acid	2.97	2.97	-
Pyrrolidine, 1-methyl-	-	-	6.12
Toluene	28.47	24.63	29.43
2,4-Dimethyl-2-oxazoline-4-methanol	6.70	8.57	5.23
Pyridine, 3-methyl-	-	-	6.29
Furfural	8.06	2.98	-
2-Pentanone, 4-hydroxy-4-methyl-	6.70	3.08	9.55
2-Furanmethanol	2.54	3.17	5.05
2,5-Furandione, dihydro-3-methylene-	-	1.63	1.78
2-Furancarboxaldehyde, 5-methyl-	5.34	4.07	-
Phenol	1.98	3.00	4.09
1,2-Cyclopentanedione, 3-methyl-	-	-	1.85
Maltol	-	1.66	2.30
Pyranone	3.51	2.30	3.86
5-Hydroxymethylfurfural	25.89	23.01	4.61
Hydroquinone	-	-	4.61
4-Hydroxy-3-methylbenzoic acid, methyl ester	-	5.80	3.34
1-Methyl-8-propyl-3,6-diazahomoadamantan-9-ol	-	2.53	2.89

Table 6. *Cont.*

Compound	Argon Flow Rate (mL·min^{-1})		
	300	150	30
	Area (%)		
9-Octadecenamide, (Z)-	-	2.92	-
Hexadecanoic acid, 2-hydroxy-ethyl ester	6.27	5.18	7.33
Octadecanoic acid, 2,3-dihydroxypropyl ester	1.57	2.50	3.25

Table 7. Compounds detected in orange pruning bio-oils chromatograms and their relative area percentages using different argon flow rates during the pyrolysis.

Compound	Argon Flow Rate (mL·min^{-1})		
	300	150	30
	Area (%)		
Pyrrolidine, 1-methyl-	1.61	-	6.91
Toluene	2.72	2.15	31.42
2,4-Dimethyl-2-oxazoline-4-methanol	-	-	5.90
3-Penten-2-one, 4-methyl-	-	1.85	-
Pyridine, 3-methyl-	-	-	3.39
2-Pentanone, 4-hydroxy-4-methyl-	89.03	94.73	10.77
2-Furanmethanol	1.46	-	5.70
2,5-Furandione, dihydro-3-methylene-	-	-	2.01
Phenol	-	-	4.62
Phenol, 2-methoxy-	1.89	-	-
Maltol	-	-	2.59
Pyranone	-	-	4.35
5-Hydroxymethylfurfural	-	-	5.20
Hydroquinone	-	-	5.20
Phenol, 2,6-dimethoxy-	1.89	-	-
Hexadecanoic acid, 2-hydroxy-ethyl ester	-	-	8.27
Octadecanoic acid, 2,3-dihydroxypropyl ester	-	-	3.67

Chromatograms using 150 and 300 mL Ar·min^{-1} showed toluene and HMF as the components of the greatest intensity and area (Table 6). Regarding the experience carried out using 30 mL Ar·min^{-1}, although the main peak also corresponded to toluene, HMF had a much smaller area and intensity. A greater number of compounds also appeared, probably because, when pyrolysis was performed at such a low Ar flow rate, a 100% inert atmosphere was not ensured. As a result, some ambient oxygen could enter the vertical tubular pyrolytic furnace, leading to the oxidation of compounds. This explanation is coherent, since, as observed in Table 6, the compounds from the experience under 30 mL Ar·min^{-1} have more oxygen in their molecular formula. Finally, furfural was found using 300 and 150 mL Ar·min^{-1}, with relative areas of 8.06% and 2.98%, respectively.

With regard to the bio-oils obtained from the pyrolysis of OP (Table 7), those resulting from pyrolysis using 300 mL and 150 mL Ar·min^{-1} contained 4-hydroxy-4-methyl-2-pentanone as the main component. However, the bio-oil produced using 30 mL Ar·min^{-1} had a wider range of compounds, in which toluene and 4-hydroxy-4-methyl-2-pentanone were the main components, the latter at a much lower concentration than in the pyrolyses using 300 mL and 150 mL Ar·min^{-1}.

Furthermore, the differences between the two raw materials were large. Orange waste produced a bio-oil with a wider range of components, while orange pruning produced a bio-oil with mainly one component: 4-hydroxy-4-methyl-2-pentanone.

3.4.3. Influence of the Heating Ramp

In order to study the influence of the heating ramp on the bio-oils obtained from OW (Table 8) and OP (Table 9) pyrolysis, the chromatograms obtained using the different heating ramps (5, 10, and 20 $^{\circ}$C$\cdot$min^{-1}) were compared, keeping the rest of the conditions constant (150 mL Ar$\cdot$min^{-1}; 400 $^{\circ}$C, 2 h).

Table 8. Compounds detected in orange waste bio-oils chromatograms and their relative area percentages using different heating ramps in the pyrolysis.

Compound	Heating Ramp ($^{\circ}$C$\cdot$min^{-1})	
	10	5
	Area (%)	
Propanoic acid	3.84	2.69
Toluene	29.43	14.85
2,4-Dimethyl-2-oxazoline-4-methanol	4.88	1.37
Furfural	8.09	8.23
2-Pentanone, 4-hydroxy-4-methyl-	5.94	13.02
2-Furanmethanol	2.71	2.04
2-Furancarboxaldehyde, 5-methyl-	6.19	6.49
Phenol	2.41	2.76
Maltol	1.31	2.37
Pyranone	2.83	9.02
5-Hydroxymethylfurfural	32.37	37.16

Table 9. Compounds detected in orange pruning bio-oils chromatograms and their relative area percentages using different heating ramps in the pyrolysis.

Compound	Heating Ramp ($^{\circ}$C$\cdot$min^{-1})		
	20	10	5
	Area (%)		
Pyrrolidine, 1-methyl-	-	-	1.82
Propanoic acid	1.68	-	-
Toluene	2.45	2.60	2.78
2-Pentanone, 4-hydroxy-4-methyl-	60.44	92.62	89.9
2-Furanmethanol	2.18	1.29	1.28
Phenol	3.63	-	-
1,2-Cyclopentanedione, 3-methyl-	3.76	-	-
Phenol, 2-methoxy-	3.81	1.24	1.56
Catechol	5.76	-	-
1,2-Benzenediol, 3-methoxy-	3.12	-	-
Phenol, 2,6-dimethoxy-	7.32	2.25	2.76
Hexadecanoic acid, 2-hydroxy-ethyl ester	2.27	-	-
Octadecanoic acid, 2,3-dihydroxypropyl ester	3.58	-	-

Bio-oils obtained from OW pyrolysis using 5 and 10 $^{\circ}$C$\cdot$min^{-1} presented as components of the highest intensity and area toluene and HMF (Table 8). The area of toluene was approximately double for the experience at 10 $^{\circ}$C$\cdot$min^{-1}, but the relative areas of HMF were quite similar, somewhat higher for that of the bio-oil obtained using 5 $^{\circ}$C$\cdot$min^{-1} heating ramp.

In the pyrolysis using the 5 $^{\circ}$C$\cdot$min^{-1} heating ramp, the third major compound found was 4-hydroxy-4-methyl-2-pentanone. In addition, both experiences had the area corresponding to furfural, their relative areas being similar and greater than 8.

It can be concluded that the main compounds present in the bio-oils obtained from OW were, regardless of the pyrolysis conditions tested, toluene and HMF, compounds that usually appear in the bio-oils of fruit residues [20,45,46] and agri-food waste [47]. The literature also corroborates the presence of furfural and phenolic compounds, among

other identified components [46]. The most suitable conditions for obtaining toluene were 10 °C·min^{-1}, 30 mL Ar·min^{-1}, and 400 °C, while the conditions for the production of HMF were 5 °C·min^{-1}, 300 mL Ar·min^{-1}, and 400 °C.

5-Hydroxymethylfurfural has been used in agrochemistry as a fungicide, in galvanochemistry as a corrosion inhibitor, in the cosmetic industry, and as a flavour agent [48]. HMF is also a starting material for the synthesis of precursors of various pharmaceuticals, thermo-resistant polymers, and complex macrocycles (2,5-furandicarbaldehyde and 2,5-furandicarboxylic acid) [48]. For this reason, OW bio-oils could be regarded as a valuable source of HMF.

Table 9 shows the main compounds found in bio-oils from orange pruning pyrolysis using different heating ramps, among which 4-hydroxy-4-methyl-2-pentanone stands out. However, its content was reduced by 30% in pyrolysis using a heating ramp of 20 °C·min^{-1}. Furthermore, the composition of the bio-oils obtained using the heating ramps of 10 and 5 °C·min^{-1} was similar. Other minor compounds such as toluene and 2-furanmethanol had the same area in the three bio-oil chromatograms. In summary, the OP bio-oils were mainly composed of 4-hydroxy-4-methyl-2-pentanone regardless of the pyrolysis conditions assayed. The most suitable conditions for obtaining this compound were 10 °C·min^{-1} heating ramp, 150 mL Ar·min^{-1} flow rate, and 600 °C pyrolysis temperature.

4-Hydroxy-4-methyl-2-pentanone is used as an intermediate in the manufacturing of dyes, inhibitors, pharmaceuticals, and insecticides and as a solvent in some industries (to adjust the solubility of paint resins and regulate the evaporation rate). It can also be used for the treatment of textiles and leather, in chemical synthesis, or as a cleaning solvent. Its current market price is 140 € per 2.5 L product (Fisher Scientific S.L., Madrid, Spain). As it can account for up to 94% of OP bio-oils (Tables 5 and 7), its production from orange pruning may be feasible.

3.5. Sulphur Removal Using Biochars from Pyrolysis of Sweet Orange Waste and Orange Pruning

Once the OW and OP biochars were obtained and characterised, the possibility of adsorbing sulphur from waste cooking oils, despite their low specific surface area, was tested. The WCO used contained a sulphur concentration of 36 mg·kg^{-1}, a concentration above the threshold indicated in the EN 14,214 and ASTM D7467 standards.

Tables 10 and 11 show the pyrolysis conditions for the obtaining of OW and OP biochars, respectively, as well as their specific surface areas and desulphurisation yields. It can be seen that the specific surface area of the OW biochars did not influence the removal of sulphur (Table 10). The highest sulphur removal (78.3%) was achieved with the biochar obtained in the pyrolysis at 400 °C, 5 °C·min^{-1}, and 150 mL·min^{-1}.

Table 10. Desulphurisation of waste cooking oil with orange waste biochars obtained under different conditions.

T (°C)	H$_{ramp}$ (°C·min^{-1})	Ar Flow (mL·min^{-1})	S$_{BET}$ (m^2·g^{-1})	Sulphur Removal (%)
400	5	150	≤1	78.3 ± 0.01
400	10	150	≤1	77.4 ± 0.03
600	10	30	≤1	76.3 ± 0.01
600	10	150	≤1	75.5 ± 0.03
600	10	300	≤1	76.2 ± 0.02

H$_{ramp}$: heating ramp; S$_{BET}$: BET-specific surface.

In contrast to OW biochars, the specific surface area of the OP biochars had an influence on the sulphur removal from waste cooking oil (Table 11). Notwithstanding, the performance of both OW and OP biochars was similar, ranging from 66.4% to 78.8%. The highest yield (78.8%) was obtained with the biochar obtained in the pyrolysis at 600 °C, 10 °C·min^{-1}, and 150 mL·min^{-1}, which had a specific surface area of 7.52 m^2·g^{-1}. The biochar obtained at 600 °C, 10 °C·min^{-1}, and 30 mL Ar·min^{-1}, despite having the largest

surface area (24.28 m^2·g^{-1}), was not the one that adsorbed the most sulphur (66.4%). Thus, there was no direct and clear relationship between the specific surface area of OP biochars and their ability to adsorb sulphur (Figure 7). The literature illustrates that the specific surface area and the pore size are inversely proportional [24]. That is, as the specific surface area increases, the pore size decreases, which could explain the obtained results.
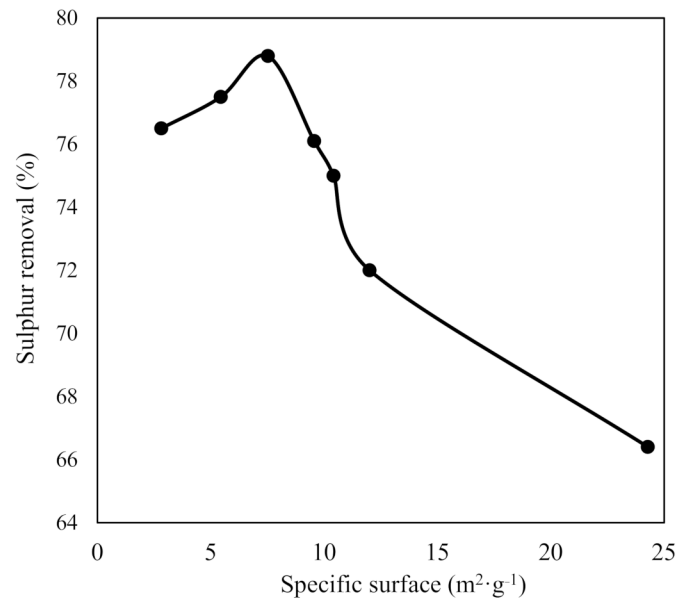

Figure 7. Effect of BET specific surface area of orange pruning biochars on sulphur removal.

Table 11. Desulphurisation of waste cooking oil with orange pruning biochars obtained under different conditions.

T (°C)	H$_{ramp}$ (°C·min^{-1})	Ar Flow (mL·min^{-1})	S$_{BET}$ (m^2·g^{-1})	Sulphur Removal (%)
400	5	150	2.82	76.5 ± 0.01
400	10	150	5.44	77.5 ± 0.03
600	10	30	24.28	66.4 ± 0.01
600	10	150	7.52	78.8 ± 0.01
600	10	300	12.01	72.0 ± 0.03
600	20	150	10.42	75.0 ± 0.04

H$_{ramp}$: heating ramp; S$_{BET}$: BET-specific surface.

A comparison was made between the FTIR spectra of the biochars that led to the highest and lowest yield in sulphur removal to assess changes in the surface compounds (Figure 8). As can be observed, two new bands appeared in the FTIR spectra after the WCO desulphurisation process. The first, at 1127 cm^{-1}, was related to the C=S bond, while the second, at 1200 cm^{-1}, was related to the O=S=O bond [49]. Finally, it should be noted that the intensity of these bands in the FTIR spectra of the biochars that led to the lowest sulphur removal yields (Figure 8B) was less intense than those of the biochars that achieved the highest sulphur removal from WCO (Figure 8A).
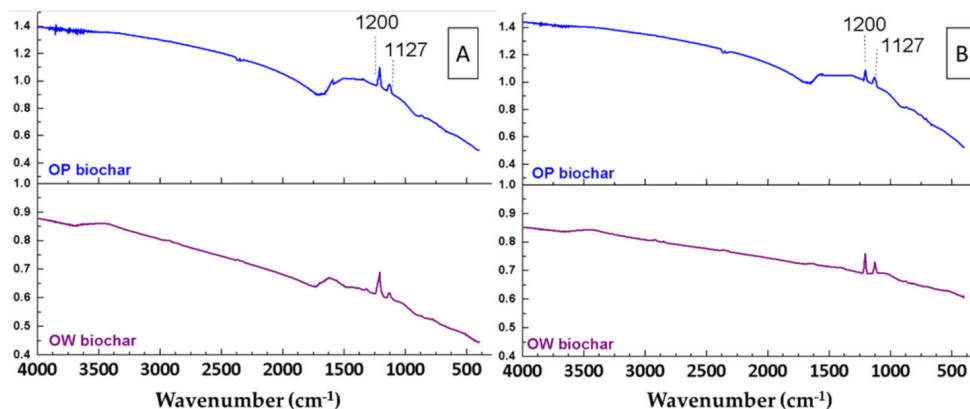
Figure 8. FTIR spectra of orange waste (OW) and orange pruning (OP) biochars after their use for sulphur removal from waste cooking oil. (**A**) Biochars that achieved the highest sulphur removal. (**B**) Biochars that achieved the lowest sulphur removal.

After all of these studies, it was clear that the most suitable OW biochar for the desulphurisation of waste cooking oils was obtained at 400 °C, 5 °C·min^{-1}, and 150 mL·min^{-1}. The OP biochar with the highest performance for the desulphurisation of waste cooking oil was obtained at 600 °C, 10 °C·min^{-1}, and 150 mL·min^{-1}.

4. Conclusions

The TGA of the raw materials showed that OP presents higher thermal stability than OW due to its higher lignin content (20% and 5%, respectively). This could also be responsible for the obtaining of higher percentages of biochar from OP than from OW when both raw materials were subjected to pyrolysis under the same conditions. The higher the pyrolysis temperature, the lower the biochar production from both raw materials. The most suitable conditions for producing biochar from the pyrolysis of OP were found to be 400 °C, 150 mL Ar·min^{-1}, and 10 °C·min^{-1}, while those for obtaining biochar from the pyrolysis of OW were 400 °C, 150 mL Ar·min^{-1}, and 5 °C·min^{-1}. The biochars produced from OP had higher specific surface area (up to 24.28 m^2·g^{-1}) than those produced from OW ($\leq$1 m^2·g^{-1}).

With regard to bio-oils, those obtained from OW were mostly composed of toluene and 5-hydroxymethylfurfural, reaching relative areas of up to 29.43% and 37.16%, respectively. By contrast, the bio-oils obtained from OP were mainly formed by 4-hydroxy-4-methyl-2-pentanone (up to 94.73% relative area).

Finally, the biochars obtained from the pyrolysis of OW and OP proved to be useful for the removal of sulphur from WCO, despite their low specific surface areas. Thus, the biochar obtained from the pyrolysis of OP at 600 °C, 150 mL Ar·min^{-1}, and 10 °C·min^{-1} achieved a reduction of 78.8% of the initial sulphur content of WCO. Similarly, the biochar obtained from pyrolysis of OW at 400 °C, 150 mL Ar·min^{-1} and 5 °C·min^{-1} led to 78.3% sulphur removal from WCO.

All in all, the results obtained in this work demonstrate that pyrolysis could be an interesting option for the treatment of OW and OP. Both the obtaining of biochars for sulphur absorption from WCO and the extraction of high-added-value compounds from bio-oils could be real, feasible alternatives for this waste.

Author Contributions: Conceptualisation, P.Á.-M.; methodology, P.Á.-M.; formal analysis, F.-J.S.-B., N.G.-C., P.Á.-M. and J.F.G.-M.; investigation, F.-J.S.-B. and N.G.-C.; resources, P.Á.-M.; writing original draft preparation, F.-J.S.-B. and J.F.G.-M.; writing review and editing, J.F.G.-M.; supervision, P.Á.-M. and J.F.G.-M.; project administration, P.Á.-M.; funding acquisition, P.Á.-M. All authors have read and agreed to the published version of the manuscript.

Institutional Review Board Statement: Not applicable.

Informed Consent Statement: Not applicable.

Data Availability Statement: The data presented in this study are available on request from the corresponding author. The data are not publicly available due to confidentiality agreements with the funding companies.

Conflicts of Interest: The authors declare that they have not known competing financial interests or personal relationships that could have appeared to influence the work reported in this paper.

References

1. FAOSTAT. Available online: http://www.fao.org/faostat/es/#data/QC (accessed on 23 May 2020).
2. Ministerio de Agricultura, Pesca y Agricultura. Superficies y Producciones Anuales de Cultivos (2017). Available online: https://www.mapa.gob.es/es/estadistica/temas/estadisticas-agrarias/agricultura/superficies-producciones-anuales-cultivos/ (accessed on 28 November 2019).
3. García-Martín, J.F.; Olmo, M.; García, J.M. Effect of ozone treatment on postharvest disease and quality of different citrus varieties at laboratory and at industrial facility. *Postharvest Biol. Technol.* **2018**, *137*, 77–85. [CrossRef]
4. Rodríguez, A.; Rosal, A.; Jiménez, L. Biorefinery of agricultural residues by fractionation of their components through hydrothermal and organosolv processes. *Afinidad* **2009**, *545*, 14–19.
5. Wilkins, M.R.; Suryawati, L.; Maness, N.O.; Chrz, D. Ethanol production by *Saccharomyces cerevisiae* and *Kluyveromyces marxianus* in the presence of orange-peel oil. *World J. Microbiol. Biotechnol.* **2007**, *23*, 1161–1168. [CrossRef]
6. Rezzadori, K.; Benedetti, S.; Amante, E.R. Proposals for the residues recovery: Orange waste as raw material for new products. *Food Bioprod. Processing* **2012**, *90*, 606–614. [CrossRef]
7. Crawshaw, R. *Co-Product Feeds: Animal Feeds from the Food and Drinks Industries*; Nottingham University Press: Nottingham, UK, 2001; p. 285.
8. Guerrero, C.C.; Carrasco de Brito, J.; Lapa, N.; Oliveira, J.F.S. Re-use of industrial orange wastes as organic fertilizers. *Bioresour. Technol.* **1995**, *53*, 43–51. [CrossRef]
9. Elías Castells, X. *Reciclaje de Residuos Industriales: Residuos Sólidos Urbanos y Fangos de Depuradora*; Ediciones Díaz de Santos, S.A.: Madrid, Spain, 2009; p. 1320.
10. Restrepo Duque, A.M.; Rodríguez Sandoval, E.; Manjarrés Pinzón, K. Edible orange peels: An approximation to the development of products with added value from agricultural products. *Producción + Limpia* **2011**, *6*, 47–57.
11. Boluda-Aguilar, M.; López-Gómez, A. Production of bioethanol by fermentation of lemon (*Citrus limon* L.) peel wastes pretreated with steam explosion. *Ind. Crops Prod.* **2013**, *41*, 188–197. [CrossRef]
12. Siles, J.Á.; Martín, M.D.L.Á.; Martín, A.; Raposo, F.; Borja, R. anaerobic digestion of wastewater derived from the pressing of orange peel generated in orange juice production. *J. Agric. Food Chem.* **2007**, *55*, 1905–1914. [CrossRef]
13. Calabrò, P.S.; Fazzino, F.; Sidari, R.; Zema, A. Optimization of orange peel waste ensiling for sustainable anaerobic digestion. *Renew. Energy* **2020**, *154*, 849–862. [CrossRef]
14. Feng, C.H.; García-Martín, J.F.; Broncano Lavado, M.; del López-Barrera, M.; Álvarez-Mateos, P. Evaluation of different solvents on flavonoids extraction efficiency from sweet oranges and ripe and immature Seville oranges. *Int. J. Food Sci. Technol.* **2020**, *55*, 3123–3134. [CrossRef]
15. Volpe, M.; Panno, D.; Volpe, R.; Messineo, A. Upgrade of citrus waste as a biofuel via slow pyrolysis. *J. Anal. Appl. Pyrolysis* **2015**, *115*, 66–76. [CrossRef]
16. Bagnato, G.; Sanna, A.; Paone, E.; Catizzone, E. Recent catalytic advances in hydrotreatment processes of pyrolysis bio-oil. *Catalysts* **2021**, *11*, 157. [CrossRef]
17. Sánchez-Borrego, F.J.; Álvarez-Mateos, P.; García-Martín, J.F. Biodiesel and other value-added products from bio-oil obtained from agrifood waste. *Processes* **2021**, *9*, 797. [CrossRef]
18. García Martín, J.F.; Cuevas, M.; Feng, C.H.; Álvarez Mateos, P.; Torres García, M.; Sánchez, S. Energetic valorisation of olive biomass: Olive-tree pruning, olive stones and pomaces. *Processes* **2020**, *8*, 511. [CrossRef]
19. Association European Biomass Industry Pyrolysis. Available online: https://www.eubia.org/cms/ (accessed on 26 May 2020).
20. Basu, P. *Biomass Gasification and Pyrolysis*, 1st ed.; Academic Press: Cambridge, MA, USA, 2010; p. 376.
21. Bhattacharjee, N.; Baran Biswas, A. Pyrolysis of orange bagasse: Comparative study and parametric influence on the product yield and their characterization. *J. Environ. Chem. Eng.* **2019**, *7*, 102903. [CrossRef]
22. Bradley, D.; Svebio, B.H.; Ab, H.; Wild, M.; Deutmeyer, M.; Schouwenberg, P.P.; Essent, R.; Hess, R.; Tumuluru, J.S.; Bradburn, K. Low Cost, Long Distance Biomass Supply Chains. In *Task 40: Sustainable International Bioenergy Trade*; Goh, C.S., Junginger, M., Eds.; IEA Bioenergy: Paris, France, 2013; pp. 1–65.

23. Encinar, J.M.; Beltran, F.J.; Gonzalez, J.F.; Moreno, M.J. Pyrolysis of maize, sunflower, grape and tobacco residues. *Chem. Technol. Biotechnol.* **1997**, *70*, 400–410. [CrossRef]

24. Wu, L.; Wan, W.; Shang, Z.; Gao, X.; Kobayashi, N.; Luo, G.; Li, Z. Surface modification of phosphoric acid activated carbon by using non-thermal plasma for enhancement of Cu(II) adsorption from aqueous solutions. *Sep. Purif. Technol.* **2018**, *197*, 156–169. [CrossRef]

25. Roy, M.; Mohanty, K. Valorization of de-oiled microalgal biomass as a carbon-based heterogeneous catalyst for a sustainable biodiesel production. *Bioresour. Technol.* **2021**, *337*, 125424. [CrossRef]

26. Sánchez-Borrego, F.J.; Barea de Hoyos-Limón, T.J.; García-Martín, J.F.; Álvarez-Mateos, P. Production of bio-oils and biochars from olive stones: Application of biochars to the esterification of oleic acid. *Plants* **2021**, *11*, 70. [CrossRef] [PubMed]

27. Álvarez-Mateos, P.; García-Martín, J.F.; Guerrero-Vacas, F.J.; Naranjo-Calderón, C.; Barrios-Sánchez, C.C.; Pérez-Camino, M.C. Valorization of a high-acidity residual oil generated in the waste cooking oils recycling industries. *Grasas Aceites* **2019**, *70*, e335. [CrossRef]

28. García Martín, J.F.; Carrión Ruiz, J.; Torres García, M.; Feng, C.H.; Álvarez Mateos, P. Esterification of free fatty acids with glycerol within the biodiesel production framework. *Processes* **2019**, *7*, 832. [CrossRef]

29. García-Martín, J.F.; Alés-Álvarez, F.J.; Torres-García, M.; Feng, C.H.; Álvarez-Mateos, P. Production of oxygenated fuel additives from residual glycerine using biocatalysts obtained from heavy-metal-contaminated *Jatropha curcas* L. roots. *Energies* **2019**, *12*, 740. [CrossRef]

30. Cárdenas, J.; Orjuela, A.; Sánchez, D.L.; Narváez, P.C.; Katryniok, B.; Clark, J. Pre-treatment of used cooking oils for the production of green chemicals: A review. *J. Clean. Prod.* **2021**, *289*, 125129. [CrossRef]

31. Shan, Y.; Erika, G.; Gray, D.; Yuan, Y.; Simeon, R. *Cost-Effective Waste to Biodiesel Production at a Wastewater Treatment Plant*; East Bay Municipal Utility District: Oakland, CA, USA, 2019.

32. Aguiar Trujillo, L.; Márquez-Montesinos, F.; Gonzalo, A.; Sánchez, J.L.; Arauzo, J. Influence of temperature and particle size on the fixed bed pyrolysis of orange peel residues. *J. Anal. Appl. Pyrolysis* **2008**, *83*, 124–130. [CrossRef]

33. Lopez-Velazquez, M.A.; Santes, V.; Balmaseda, J.; Torres-Garcia, E. Pyrolysis of orange waste: A thermo-kinetic study. *J. Anal. Appl. Pyrolysis* **2013**, *99*, 170–177. [CrossRef]

34. Aburto, J.; Moran, M.; Galano, A.; Torres-García, E. Non-isothermal pyrolysis of pectin: A thermochemical and kinetic approach. *J. Anal. Appl. Pyrolysis* **2015**, *112*, 94–104. [CrossRef]

35. Álvarez-Mateos, P.; Alés-Álvarez, F.J.; García-Martín, J.F. Phytoremediation of highly contaminated mining soils by *Jatropha curcas* L. and production of catalytic carbons from the generated biomass. *J. Environ. Manag.* **2019**, *231*, 886–895. [CrossRef]

36. Yang, H.; Yan, R.; Chen, H.; Lee, D.H.; Zheng, C. Characteristics of hemicellulose, cellulose and lignin pyrolysis. *Fuel* **2007**, *86*, 1781–1788. [CrossRef]

37. Martínez-Cartas, M.L.; Sánchez, S.; Cuevas, M. Thermal characterization and pyrolysis kinetics of six types of tropical timber from Central Africa. *Fuel* **2022**, *307*, 121824. [CrossRef]

38. Miranda, R.; Bustos, D.; Sosa Blanco, C.; Gutiérrez Villarreal, M.H.; Rodriguez Cantú, M.E. Pyrolysis of sweet orange (*Citrus sinensis*) dry peel. *J. Anal. Appl. Pyrolysis* **2008**, *86*, 245–251. [CrossRef]

39. Monteiro Santos, C.; Dweck, J.; Silva Viotto, R.; Henrique Rosa, A.; de Morais, L.C. Application of orange peel waste in the production of solid biofuels and biosorbents. *Bioresour. Technol.* **2015**, *196*, 469–479. [CrossRef] [PubMed]

40. Abdelaal, A.; Pradhan, S.; Al-Nouss, A.; Tong, Y.; Al-Ansari, T.; McKay, G.; Mackey, H.R. The impact of pyrolysis conditions on orange peel biochar physicochemical properties for sandy soil. *Waste Manag. Res.* **2021**, *39*, 995–1004. [CrossRef] [PubMed]

41. Del Pozo, C.; Rego, F.; Yang, Y.; Puy, N.; Bartrolí, J.; Fàbregas, E.; Bridgwater, A.V. Converting coffee silverskin to value-added products by a slow pyrolysis-based biorefinery process. *Fuel Processing Technol.* **2021**, *214*, 106708. [CrossRef]

42. Charusiri, W.; Vitidsant, T. Biofuel production via the pyrolysis of sugarcane (*Saccharum officinarum* L.) leaves: Characterization of the optimal conditions. *Sustain. Chem. Pharm.* **2018**, *10*, 71–78. [CrossRef]

43. Lugo, C.; García, E.; Rondón, J.; Briceño, J.; Pérez, P.; Rodríguez, P.; del Castillo, H.; Imbert, F. Study of reactions catalyzed as methane reforming and selective catalytic reduction of nox on perovskites of Type $La_{0.7}Sr_{0.3}Ni_{1-X}Co_xO_3$ obtained via SCS. Part II. *Rev. Cienc. Ing.* **2020**, *41*, 35–146.

44. De Almeida, C.F.; de Andrade, R.C.; de Oliveira, G.F.; Suegama, P.H.; de Arruda, E.J.; Texeira, J.A.; de Carvalho, C.T. Study of porosity and surface groups of activated carbons produced from alternative and renewable biomass: Buriti petiole. *Orbital* **2017**, *9*, 18–26. [CrossRef]

45. Kim, J.W.; Lee, S.-H.; Kim, S.-S.; Park, S.H.; Jeon, J.-K.; Park, Y.-K. The pyrolysis of waste mandarin residue using thermogravimetric analysis and a batch reactor. *Korean J. Chem. Eng.* **2011**, *28*, 1867–1872. [CrossRef]

46. Özbay, N.; Apaydın-Varol, E.; Burcu Uzun, B.; Eren Pütünb, A. Characterization of bio-oil obtained from fruit pulp pyrolysis. *Energy* **2008**, *33*, 1233–1240. [CrossRef]

47. Van de Beld, B.; Funke, A.; Lindfors, C.; Sandström, L. Country Reports 2019. In *Task 34: Direct Thermochemical Liquefaction*; Funke, A., Ed.; IEA Bioenergy: Paris, France, 2019; pp. 1–20.

48. Lewkowski, J. Synthesis, chemistry and applications of 5-hydroxymethylfurfural and its derivatives. *Arkivoc* **2001**, *1*, 17–54. [CrossRef]

49. Huang, S.; Liang, Q.; Geng, J.; Luo, H.; Wei, Q. Sulfurized biochar prepared by simplified technic with superior adsorption property towards aqueous Hg(II) and adsorption mechanisms. *Mater. Chem. Phys.* **2019**, *238*, 121919. [CrossRef]